Characterization of an LSO scintillator for space applications

Journal of Physics: Conference Series **632** (2015) 012006 doi:10.1088/1742-6596/632/1/012006

Characterization of an LSO scintillator for space applications

R Elftmann, J Tammen, S R Kulkarni, C Martin, S Böttcher, R Wimmer-Schweingruber

Institute of Experimental and Applied Physics, University of Kiel, Leibnizstr. 11-19, D-24118 Kiel, Germany

E-mail: elftmann@physik.uni-kiel.de

Abstract. Currently BGO ($Bi_4Ge_3O_{12}$) is widely used for the detection of high-energy particles in space applications because of its high stopping power, the non-hygroscopic characteristics and its ruggedness with respect to mechanical stress. The new Cerium doped LSO (Lu_2SiO_5) offers the same benefits with higher light output capabilities and a significantly shorter decay time. We investigated key characteristics of an LSO scintillator in view of its use in space missions. We characterized the intrinsic spectrum which originates from the decay of ^{176}Lu and showed that it consists of three different parts arising from different effects: the native intrinsic spectrum, chance coincidence effects and energy deposition in the readout photodiode. Furthermore we investigated the light-quenching of LSO for heavy ions with measurements performed at the Heavy Ion Medical Accelerator in Chiba (HIMAC), Japan. We found that LSO is a promising candidate for future space missions.

1. Introduction

Scintillators have been used for the detection of energetic particles since the beginning of the 20th century. Because scintillation materials differ in characteristics such as light output, ruggedness, density, or atomic number the search for the ideal scintillator is not finished. Many new materials have been discovered and developed in recent years and one of these materials was Lu_2SiO_5:Ce (LSO) [3]. Since its development it has widely replaced BGO in Positron Emission Tomography (PET) scanners because of its higher light output and shorter decay time of 42 ns compared to 300 ns of BGO. Table 1 gives a comparison between commonly used inorganic scintillation materials and LSO.

For the detection of high energy particles in space, a scintillation material with high density and high atomic number is attractive because this reduces the volume of stopping material and thus the required volume and mass of the instrument. Therefore BGO as well as LSO are both suitable candidates for these applications. While BGO is already used in various space applications LSO has not been used so far. Before LSO can be used for space applications necessary key characteristics have to be investigated like the response to heavy particles, temperature dependence of light output or the effects of the high inherent radioactivity. LSO contains a significant amount of ^{176}Lu atoms, which decay to ^{176}Hf via β^- -decay emitting three main gamma lines as shown in fig. 1. These gamma lines are almost emitted in coincidence so that all gamma lines or combinations thereof may be detected at the same time. Moreover the high amount of ^{176}Lu leads to a high intrinsic decay rate and therefore to a significant background.

	NaI(Tl)$^\diamond$	BGO$^\diamond$	GSO(Ce)$^\diamond$	LSO(Ce)$^\diamond$	CsI(Tl)†
Density (g/cm^3)	3.67	7.13	6.7	7.4	4.51
Effective atomic number	51	75	59	66	54
Radiation length (cm)	2.56	1.12	1.38	1.14	1.85
Hygroscopic	yes	no	no	no	Slight
Rugged	no	yes	no	yes	yes
Refractive index	1.85	2.15	1.85	1.82	1.80
Relative light intensity	100	15	25	75	145
Decay constant (ns)	230	300	56, 600	40	1220
Peak Wavelength (nm)	410	480	440	420	560

Table 1. Properties of common inorganic scintillation materials. $\diamond$ taken from [4], † from [1],[2].

The higher light output of LSO compared to BGO is only determined for low ionizing particles. Heavy ionizing particles introduce an additional non-linear light loss mechanism, known as ionization quenching [7], which is different for each scintillation material and varies with the particle energy and species. This light loss mechanism is related to the high density of excited states within the scintillation detector which is produced by the heavy ionizing particles. The quenching factors for LSO have to be determined to clarify whether the light output of LSO is also superior for heavy particles and to calculate the real deposited energies of heavy particles detected with LSO.

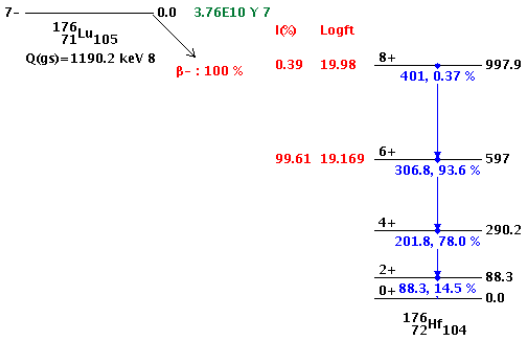

Figure 1. Decay scheme of ^{176}Lu. This isotope has an abundance of 2.59%. Taken from [5].

2. Characterization of the intrinsic spectrum of LSO:Ce

The intrinsic spectrum of LSO arises from the β^- -decay of ^{176}Lu. In order to determine the origin of different parts of the resulting spectrum, we compared a measured spectrum to a Geant4 simulation.

The LSO crystal we used for our characterization was manufactured by Scionix Holland with a Cerium doping level of 0.5%. The dimensions were 3 x 1.5 x 1 cm^3 and the crystal was initially completely polished. The readout of the scintillator was performed using a Hamamatsu Photonics PIN photodiode model S-3590-19 which was glued to one half of the 3 x 1.5 cm^2 side of the scintillator. For the glueing Dow Corning 93-500 Space-grade encapsulant was used. The S-3590-19 offers an enhanced sensitivity in the blue light region and matches the emission spectrum of LSO quite well. In order to increase optical coupling with the photodiode, the crystal surface where the photodiode was glued was roughened. The complete scintillation detector was wrapped with one layer of Millipore and two layers of PTFE tape to increase the light collection.

A picture of the scintillation detector is shown fig. 2 a). The signal of the photodiode was pre-amplified using a space grade charge-sensitive preamplifier which was designed and produced at our institute. The signal was further amplified by an Canberra amplifier model 2022 with 2 μs shaping time and the pulse height was measured with a Fast Comtec multiparameter system MPA-3. The calibration of the scintillation detector was performed with a ^{207}Bi and a ^{60}Co source.
We recorded the intrinsic spectrum of LSO for 3 hours and the result is shown as the red line in

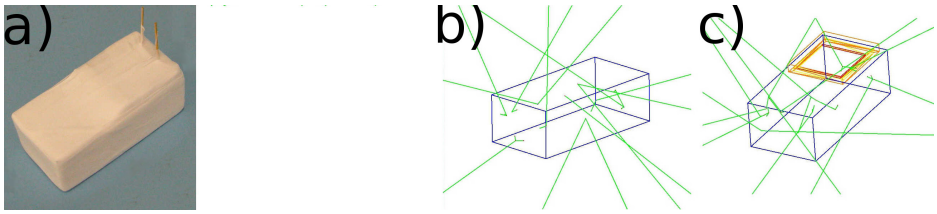

Figure 2. a): wrapped LSO scintillation detector. b): illustration of the first simulation model. c): the complete simulation model with the photodiode. The light green lines represent sample gamma trajectories.

fig. 3. With the calibrated intrinsic spectrum, shown in fig. 1, we can show that the energy range is higher than the expected Q-value of 1190.2 keV. To clarify the origin of the higher energy part of the spectrum a Geant4 simulation was performed using the Radioactive Decay module. With this module it is possible to accurately simulate the radioactive decay of unstable isotopes and to track the resulting particles.
The first approach for the simulation was to simulate the decay of ^{176}Lu and evaluate only the deposited energy in the crystal. The complete crystal was defined as a source volume so that unstable ^{176}Lu atoms were randomly distributed throughout the complete crystal. To compare the intensity of the simulation with that of the experiment, the number of decays during the time of the experiment had to be estimated. The amount of ^{176}Lu atoms in the crystal was approximated by using the mass of the crystal and the mass of a single LSO primitive cell. The decay rate can then be calculated to 1277 Bq taking into account the half life of the isotope. This rate is in good agreement with the rate of 300 $\frac{\text{Bq}}{\text{cm}^3}$ found in previous experiments [6]. Because the scintillation detector has a limited resolution and other line broadening effects it was necessary to introduce noise into the simulated spectrum. Therefore Gaussian noise with a σ of 30 keV was applied to the simulated spectrum. The simulated spectrum where only energy deposition in the crystal was taken into account is shown as the magenta line in fig. 3. The direct comparison between simulation and measurement shows a good agreement up to ≈1100 keV. Up to this energy the intensity as well as the position of the peaks match the experiment. However, while the simulated spectrum ends at 1190 keV the measured spectrum extends to energies above 4000 keV. Therefore it appears that high energy events which were measured in the experiment can not be attributed to direct energy deposition in the crystal by the intrinsic radiation.
By introducing two effects in the simulation the origin of the high energy events can be explained. The first effect is known as chance coincidence and results from the high intrinsic decay rate and the shaping time of 2 μs of the shaper. The rate r of the these events can be calculated as shown in eqn. 1 with the activity of the crystal r_{source} of 1277 Bq and the shaping time τ of 2 μs to be 3.26 s^{-1}. When we consider the chance coincidence events in the evaluation of the simulation, we can explain the first part of the high energy events as shown in blue line in fig. 3. The energy range of the simulated spectrum extends up to ≈2000 keV and the shape of this part matches the shape of the measured spectrum. The reason for the deviation of the spectra

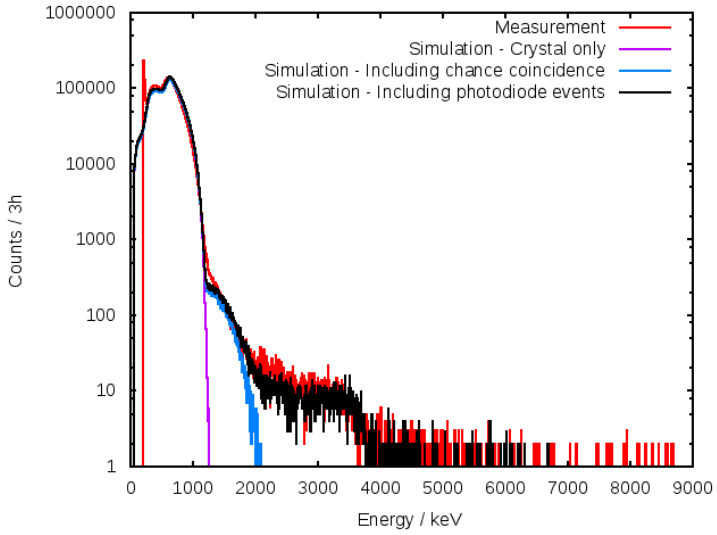

Figure 3. The red graph shows the measured intrinsic spectrum of LSO. If only energy deposition in the crystal is considered in the simulation the maximum energy is 1190 keV (magenta graph). Considering the chance coincidence counts in the simulation leads to a better match of the simulated and measured spectrum (blue graph). Photodiode hits introduce a high energy part into the intrinsic spectrum (black graph).

in the energy range between 1400 keV and 1500 keV is most probably the simple model we applied instead of the exact process of the measurement system. The electronics are sensitive to temporal separation of events within the shaping time interval and that alters the total height of the resulting peak. Thus the double events are shifted towards lower energies in the real measurement and that explains the deviation between the two spectra in that region. The consideration of these chance coincidence events is important for LSO because of its high intrinsic decay rate. Especially when large scintillator volumes are used these events will significantly influence the spectrum since the rate of double events is proportional to the single event rate squared.

$$r = (r_{source})^2 \cdot \tau \tag{1}$$

The second effect which leads to the generation of high energy events is direct energy deposition in the readout photodiode of the scintillation detector. To study these events we implemented the photodiode and the glue which was used to glue the photodiode to the crystal in the simulation. The conversion efficiency of the photodiode is superior to that of LSO. Therefore events where the photodiode is hit by primary particles produce a higher electronic signal which is converted to higher energies when using the LSO calibration. In order to take this effect into account for the simulation the deposited energy in the photodiode had to be multiplied by a conversion factor. We determined the conversion factor with the same experimental setup as used before with a photodiode of the same model as used for the LSO readout. By comparing the two calibration functions we determined the conversion factor from photodiode to LSO to be 18.6. This factor was applied to the energy which was deposited in the photodiode in the simulation. The black line in fig. 3 shows that the last part of the intrinsic spectrum can be reconstructed using this approach. This part of the simulated spectrum matches not only the shape of the experimental spectrum but also the maximum energy. We found that the spectrum in the photodiode is almost exclusively created by electrons which pass through the glue and deposit energy in the silicon.

These events can be rejected by using a second readout photodiode. However, this results in a loss of resolution so that for high resolution applications these events should be considered.

3. Determination of quenching factors

Quenching is known as an non-linear light-loss of scintillation light [7]. To determine the quenching factors for LSO we designed and built a particle telescope consisting of the previously used LSO crystal, one 2 x 2 x 2 cm^3 BSO scintillator, an anti-coincidence photodiode between the scintillators and two tracking photodiodes. A CAD view of the instrument is shown in fig. 4. Both scintillators were wrapped in two layers of Millipore and PTFE tape. To detect the scintillation light of the scintillators each scintillator was read out by two photodiodes. Therefore events where a photodiode is directly hit by a particle can be excluded from the analysis. The telescope features two entrance windows, so that ions may enter the instrument from two sides. This makes a individual characterization of each scintillator possible. Measurements of the scintillator response to several heavy ion species were performed at the **H**eavy **I**on **M**edical **A**ccelerator in **C**hiba (HIMAC), Japan. In this work we present the quenching factors of LSO

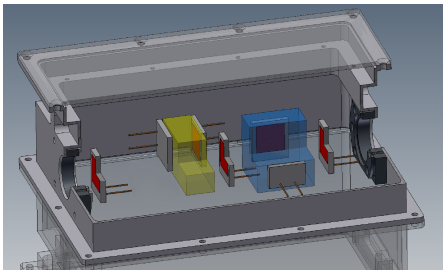

Figure 4. The LSO crystal is shown in yellow, the BSO in blue. Circular openings at the ends allow an individual characterization of each scintillator.

for He, C, and Si. The initial energies of these ions at HIMAC are 230 MeV/nuc, 400 MeV/nuc and 800 MeV/nuc, respectively. By placing polyethylene (PE) blocks in front of the telescope we were able to decrease the ion energy. The instrument was calibrated using protons which originate from ion fragmentation processes of the primary ions inside the PE absorber and also with cosmic muons. The muons and the protons both produce only low ionization densities inside the scintillator and thus they do not exhibit quenching and can be used for calibration. Figure 5 shows the combined measurement data points for all He measurements for the various PE thicknesses. The deposited energy in the crystal is plotted against the deposited energy in the photodiode. With increasing PE thickness, the deposited energy in the LSO increases up to a certain value until at a certain thickness the particles stop in the scintillator. At this point the deposited energy decreases since the particles only deposit their remaining energy. The quenching is most severe for stopping particles because of the high dE/dx, especially at the Bragg peak. In order to determine the quenching factors for LSO we utilize Birks empirical quenching formula, equation 2, for the light output of a scintillator per path length, dL/dx, which takes into account the effect of quenching. B·dE/dx gives the ionization density of molecules along the track and with the quenching parameter k, kB gives the amount of molecules which contribute to quenching. S is the scintillation efficiency [7].

$$\frac{dL}{dx} = \frac{S\frac{dE}{dx}}{1 + kB\frac{dE}{dx}} \tag{2}$$

Using eqn.2 and the approximation for high energetic particles that dE/dx $\approx \frac{CAZ^2}{E}$ [8] with C being a proportionality constant the following equation can be calculated:

$$L(E) = C_1 \left(E - C_2 A Z^2 \ln \left| \frac{E + C_2 A Z^2}{C_2 A Z^2} \right| \right) \tag{3}$$

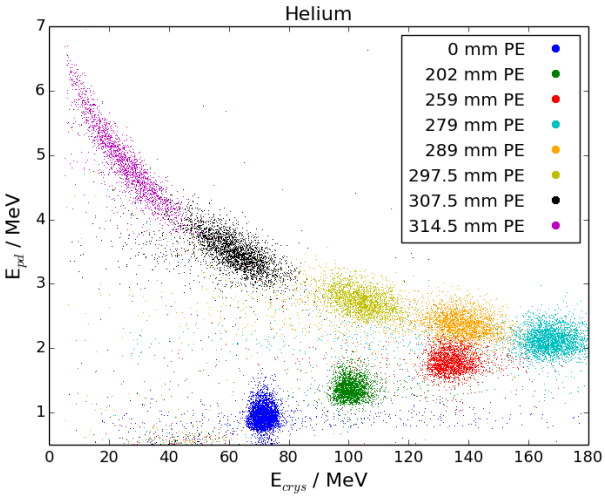

Figure 5. The measured and calibrated data points of the helium run. The data are not corrected for quenching.

The deposited energy E was calculated with a Geant4 simulation of the complete setup at HIMAC. With the energy E and the atomic mass and charge number, A and Z, we determined the parameters C_1 and C_2. For L we used the deposited energy from the measurement. Therefore the resulting quenching factors are not related to the light output of the scintillator and can be compared to other scintillators more easily. Furthermore the results can be applied to any calibrated LSO scintillation detector. For each PE thickness and ion species the most probable energy loss in the LSO and in the photodiode was determined with a fit of a 2-D Gaussian function. This was done for the simulation as well as for the experiment. The most probable energy loss in LSO of the measurement and of the simulation were then plotted against each other in fig. 6 to determine the quenching factors. The quenching parameters were determined by a least square fit of eqn. 3 to the data points of the ions which stop in the LSO crystal. For each ion species a separate set of parameters was determined. The parameter C_1 is proportional to the scintillation efficiency S and the parameter C_2 is proportional to the quenching factor kB. In our case the scintillation efficiency, parameter C_1, is particle specific and thus determined for each ion individually. The resulting curves from the least square fit are displayed in fig. 6. For illustration a dotted line is added to the plot where the measured energy E_{meas} of the experiment is the same as the simulated energy E_{sim}. This line shows where one would expect the peaks to lie of no quenching occurs. As expected the light loss due to quenching increases with the atomic mass and charge number of the ion.
Sources of experimental errors are a possible tilt in the adjustment, a non exact thickness or a density uncertainty of the PE. We considered these uncertainties by performing worst-case simulations and used the deviations from our determined values as error approximations. The uncertainty of the simulation was taken as 1% as given in [9] and [10] for the accuracy of Geant4 simulations for energy loss by ionization. The uncertainty from the determination of the most probable energy loss from the fit of the 2-D Gaussian was also taken into account for the experiment and the simulation. The resulting parameters for C_1 and C_2 are given in tab. 2. With these

quenching factors it is possible to calculate the correct deposited energy for any calibrated LSO scintillation detector for the investigated ion species. While the errors for the C_1 parameters are below 4%, the errors of the C_2 parameters are quite large. The bending of the curve at low energies which is mostly described by this parameter C_2 needs more data points in order to be determined more accurately.

Ion	C_1	C_2 / MeV
He	0.712 ± 0.029	0.084 ± 0.043
C	0.529 ± 0.015	0.043 ± 0.005
Si	0.348 ± 0.014	-0.00055 ± 0.00035

Table 2. The parameters C_1 and C_2 of eqn. 3 obtained from the least square fit for each ion species.

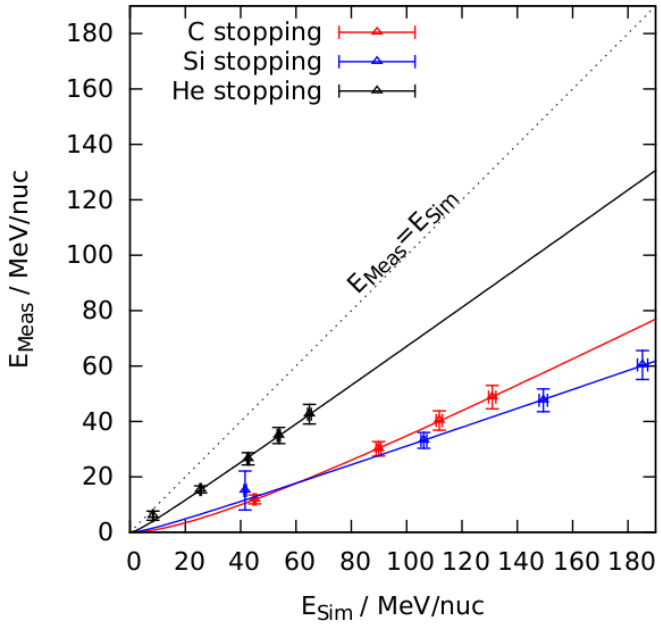

Figure 6. The energy deposited of the ions stopping in the LSO from the experiment and from the simulation is plotted against each other. For each ion species an individual fit is performed using eqn. 3.

Similar studies have been performed with the same method for BGO [11] and so we are able to compare those results with these for LSO. LSO has a five times higher light emission for light particles compared to BGO but is also known as a heavy quencher [2]. By comparing our results with BGO we can show that despite the higher quenching, the light output of LSO is superior to that of BGO for heavy ions, at least for the investigated ion species. Table 3 shows the C_1 parameter of LSO and that of BGO taken from [11]. The relative scintillation efficiencies of LSO are always lower than those of BGO. This means that a higher amount of energy is lost to quenching in LSO. However, because LSO produces five times more photons per MeV compared to BGO, LSO still emits 3.0 ± 1.2 times more light for C, 3.6 ± 1.4 times more light for He and 3.6 ± 1.2 more light for Si. Therefore LSO is indeed suited for the detection of heavy ions in future space missions and promises an increased resolution and a better signal to noise ratio. For measurements of high energy particles the intrinsic spectrum is not problematic because its maximum energy is below 4 MeV.

Ion	$S_{spec,BGO}$	$S_{spec,LSO}$	$S_{spec,LSO}/S_{spec,BGO}$	Light output
He	0.987 ± 0.202	0.712 ± 0.029	0.722 ± 0.289	3.608 ± 1.415
C	0.878 ± 0.078	0.529 ± 0.015	0.603 ± 0.239	3.013 ± 1.194
Si	0.480 ± 0.059	0.348 ± 0.014	0.726 ± 0.231	3.628 ± 1.154

Table 3. The specific scintillation efficiencies for BGO and LSO. The light output is the ratio between the specific scintillation efficiencies multiplied by a factor of 5. This factor is the difference in light output between BGO and LSO [4]. The values for BGO are taken from [11].

4. Summary

We have characterized the intrinsic spectrum of LSO:Ce resulting from the β^--decay of ^{176}Lu as measured with a photodiode glued to the LSO crystal. By comparing the intrinsic spectrum with a Geant4 simulation we could identify three parts in the spectrum originating from three different sources. The first part is the native intrinsic spectrum with an energy range up 1192 keV and the highest intensity. This part is found in all LSO scintillation detectors. The second part originates from an electronic effect known as chance coincidence and ranges up to $\approx$ 2000 keV. The intensity of this part is highly sensitive to the size of the scintillator and the shaping time of the electronics. The last part of the spectrum results from electrons which leave the crystal and deposit energy directly in the silicon of the photodiode. The crystal we used for the investigation showed a decay rate of 306 $\frac{\mathrm{Bq}}{\mathrm{cm}^3}$. This high intrinsic decay rate limits the use of large LSO scintillators because of the chance coincidences. Furthermore we could show that photodiode hits need to be considered for an accurate characterization of LSO.
For the second part of the characterization we build a complete particle telescope containing an LSO scintillator and performed heavy ion measurements at the HIMAC, Japan. With these we determined the quenching factors of He, C, and Si, such that the correct deposited energy of these ion species can be calculated for any calibrated LSO scintillation detector. A comparison with the currently used scintillation material BGO shows that despite the higher quenching the light emission of LSO is still at least a factor of three superior to BGO.

5. Acknowledgements

We thank the NIRS-HIMAC team for the opportunity to perform research with their accelerator, and their Accelerator Engineering Corporation (AEC) for smooth beam times.

References

[1] Saint-Gorbain Crystals 2014 http://www.crystals.saint-gobain.com/
[2] Avdeichikov V V et al 1994 Light output and energy resolution of CsI, YAG, GSO, BGO and LSO scintillators for light ions. J. Nucl. Instr. Meth. Phys. **349.1** 216-224
[3] Derenzo S E et al 2003 The quest for the ideal inorganic scintillator J. Nucl. Instr. Meth. Phys. A **505** 111-117
[4] Melcher C L and Schweitzer J S 1992 Cerium-doped lutetium oxyorthosilicate: a fast, efficient new scintillator J. IEEE Trans. Nucl. Sci. **39.4** 502-505
[5] National Nuclear Data Center 2014 http://www.nndc.bnl.gov/nudat2/
[6] Ludziejewski T et al 1995 Advantages and Limitations of LSO Scintillator in Nuclear Physics Experiments J. IEEE Trans. on Nucl. Sci. **42(4)** 328336
[7] Birks J B 1964 The theory and practice of scintillation counting
[8] Horn D et al 1992 The mass dependence of CsI (Tl) scintillation response to heavy ions J. Nucl. Instr. Meth. Phys. A **320.1** 273-276
[9] Amako K et al 2005 Comparison of Geant4 electromagnetic physics models against the NIST reference data J. IEEE Trans. Nucl. Sci. **52.4** 910-918
[10] Giani S et al 1999 Geant4 simulation of energy losses of ions INFN/AE-99/21
[11] Tammen J 2013 Scintillation efficiency of BGO Technical report Institute for experimental and applied physics, University of Kiel